

Application of 3D Numerical Model and Intelligent Systems in Discharge Coefficient Estimation of Combined Weir-Gate

Nima Aein^{a, *}, Mohsen Najarchi^{a, **}, Seyyed Mohammad Mirhosseini Hezaveh^a,
Mohammad Mehdi NajafiZadeh^b, and Ehsanollah Zeighami^a

^aDepartment of Civil Engineering, Arak Branch, Islamic Azad University, Arak, 7186737869 Iran

^bDepartment of Mechanical Engineering, Arak Branch, Islamic Azad University, Arak, 3818145687 Iran

*e-mail: n.aein84@gmail.com

**e-mail: m-najarchi@iau-arak.ac.ir

Received April 14, 2019; revised August 30, 2019; accepted August 30, 2019

Abstract—Combined weir-gate structure is one of the important structures which are control the water level, measure discharge and avoid sediment deposition behind the weir. In this study, first try to simulate four combined triangular weir-rectangular gates with different geometric conditions via 3D numerical software (Flow-3D) by using experimental data. Then, dimensionless analyses were done to find the non-dimension parameters affected the discharge coefficient of this structure. At the end, four different intelligent system models were used to estimate the discharge coefficient, evaluated and compared the results with each other. Results show that the Flow-3D software has a high capability to simulate the flow over the combined structure. Besides, the values of goodness of fit criteria show that the numerical solver, estimate the water head and discharge coefficient very well. Moreover, in all models, the results show that the discharge coefficient has an inverse relation with dimensionless parameters (h/b , h/d and h/y) and discharge coefficients in this study are between 0.3–0.9. On the other hand, results of accuracy analyses of four intelligent system models of MLP, RBF, GRNN and M5P show that the MLP model is the superior model in this study, and after that, the rest of models' sort as M5P, RBF and GRNN in this study.

Keywords: combined triangular weir-rectangular gate, Flow-3D, intelligent system, MLP, RBF, GRNN, M5P

DOI: 10.1134/S0097807820040028

INTRODUCTION

Discharge estimation or measurement is one of the most important topics in all fields related to hydraulic and waterways. In this regards, so many researchers try to develop and present methods for estimating discharge. Among these researchers, few researches are based on the direct measurement of velocity such as floating objects, velocity meter (i.e. electromagnetic probes) and etc.; few researches are based on the measuring the water head over the hydraulic structures by making the control section (i.e. using weirs and etc.); few researches are based on the optimization methods and solving the flow equations; and few researches are based on the remote sensing and satellite images. Among these mentioned researches from past till now, using the hydraulic structures and making the control section is always interesting and useful for engineers due to the simplicity, accuracy and applicability of this method. Hence, few hydraulic structures were used separately in the natural and synthetic waterways such as weirs, slots, gates, parshall-flume and etc. which they have their own advantages and drawbacks. One

hydraulic structure which is interesting for engineering and researchers in recent decade is combined structure of weir and gate.

Combined weir-gate structure has the advantages of both weir and gate. This important and useful structure can control the water head in the water way, measure the flow rate pass over/through the combined structure, avoiding the sedimentation behind the weir by passing the sediment from the gate and etc. Before 1985, there is low information of using this combined weir-gate structure; till Ahmad [2] studied the combination of rectangular weir with a rectangular gate. Ahmad [2] tried to find a discharge coefficient for this combined structure. However, his try is not successful due to the lack of sufficient data [25]. Then, few experimental studies were done to evaluate the combined weir-gate structure. Negm et al. [27] investigated the effect of geometry parameters on combined rectangular weir with inverse triangular gate with angle of 45° to 110° . Negm [25] evaluated the characteristic of free flow over the combined rectangular weir- contracted rectangular gate; and presented a regression equation for estimating discharge coefficient. El-Saiad et al.

[16] evaluated the flow measurement of combined flow from low to high discharge for rectangular weir and triangular gate with angle of 45° to 124° . Besides, they present an equation for estimating discharge for the mentioned combined weir-gate. Alhamid et al. [3] evaluated the combined flow in the submerged condition, and presented an equation for their specific conditions. Similar to the Alhamid et al. [3], Negm et al. [28] investigated the effect of downstream submergence on the flow discharge of rectangular weir-triangular gate. They showed that submergence ratio of gate, effect the upstream water depth and flow discharge. This effect is somehow that by increasing the downstream submergence, the upstream water depth and flow discharge increased. Alhamid et al. [3] showed that in arid and semi arid areas, the combined structure has high efficiency and it can passed more suspended and bed load sediment. More details about bed load exist in the literature [5, 10].

Study of combined weir-gate structure still is interesting for researchers in recent decades, such as Ferro [18] is presented an equation for estimating discharge for flow over and under the broad rectangular gate based on the dimensional analyses. Negm et al. [26] are experimentally evaluated the combined rectangular weir-gate structure for various conditions such as different geometry, different bed slope of channel and etc.; and finally, they represent an equation for all geometry and hydraulic conditions. Dehghani et al. [15] are investigated the dimension of downstream scouring of combined weir-gate structure. Mohamed et al. [24] are introduced a new appearance of combined weir-gate which is a combination of broad rectangular weir without any contraction and three small pipes as a gate. They used the energy equation and dimensional analyses to show the efficiency of their structure. Balouchi and Rakhshanderoo [9] are experimentally evaluated the discharge coefficient of combined rectangular weir-triangular gate for various hydraulic and geometric conditions.

On the other hand, due to the high efficiency of intelligent systems for predicting the non-linear and complex problems, researchers interested to use these models. Among the studies that used intelligent systems regarding to hydraulic structures, below studies can be found. Bilhan et al. [12] and in the similar study Emiroghlu et al. [17], are evaluated the efficiency of artificial neural network to estimate discharge coefficient of side weirs. Their results showed that the artificial neural network models have better results than linear and non-linear regression models. Juma et al. [20] used and evaluated the efficiency of Multy Layer Perceptron (MLP) model to estimate discharge coefficient of semi-circular weirs.

Present study, try to evaluate the efficiency of Flow-3D software for simulating the flow over the combined triangular weir-rectangular gate in three dimensions and compute the discharge coefficient of

this important structure. Then, using four intelligent system models to evaluate and compare the efficiency of these models. Hence, this paper consists of four parts. The second part is materials and methods which explained about the experimental and numerical methods and intelligent systems used in this study. The third part is discussion of results which discussed about the results obtained from 3D numerical simulation and intelligent systems results. The last section is conclusion which specifies the concluding remarks of results.

MATERIALS AND METHODS

Physical Modeling

The experimental part of this study was done in the hydraulic laboratory of Shahid Chamran University of Ahwaz, Iran [9]. The experimental sides of flume made with glass; and the length, width and height of the flume are 12, 0.25, and 0.5 m, respectively. The models are made with Plexiglas which the schematic of them and the involved parameters are shown in Fig. 1. The angle of triangular weir used in the Balouchi and Rakhshanderoo [9] models are constant and equal to 60° .

Dimensionless Analysis

In order to find the effective dimensional parameters of triangular weir-rectangular gate of this study, Buckingham-theory were used. In this study, twelve independent parameters with three main quantities (length, mass and time) were considered. After following the steps of dimensional analyses, nine dimensionless parameters extract which show in Eq. (1).

$$f\left(Re, We, Fr, \theta, \frac{Q_t}{\sqrt{gh}^{2.5}}, \frac{h}{d}, \frac{h}{y}, \frac{h}{b}, \frac{h}{B}\right). \quad (1)$$

In which Re , We and Fr are Reynolds, Weber and Froude number, respectively. Q_t is the total discharge of combined structure and other parameters show in Fig. 1. It should be noted that B and θ are constant in this study. As the water diameter over the structure is high enough, the effect of surface tension (Weber number) can be ignored. Besides, as the Reynolds number is high, the effect of viscosity (Reynolds number) can also be ignored. According to the rules of dimensional analysis, the effect of velocity (and consequently Froude number) is the same as discharge and can be replaced with each other. Hence, the Froude number can be ignored in the Eq. (1). Moreover, one might name the term of $\frac{Q_t}{\sqrt{gh}^{2.5}}$ as the dimensionless discharge or discharge coefficient (C_d).

Therefore, Eq. (1) can be shortened to Eq. (2) as follows:

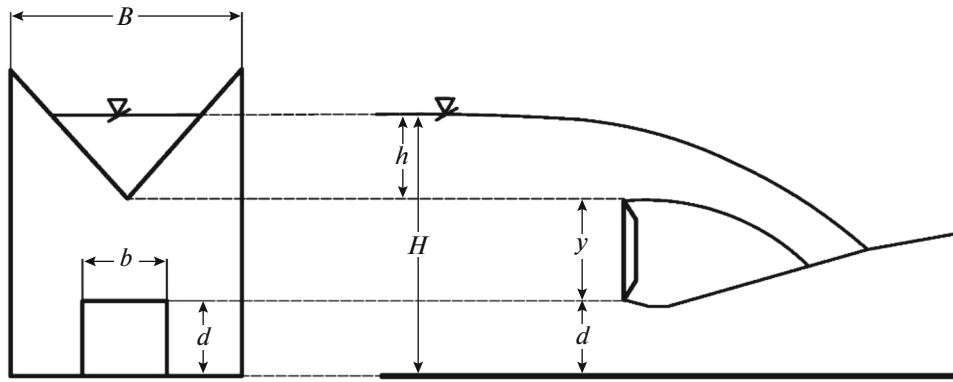


Fig. 1. Schematic of combined weir-gate structure [9].

$$q_L = Cd = \frac{Q_t}{\sqrt{gh^{2.5}}} = f\left(\frac{h}{d}, \frac{h}{b}, \frac{h}{y}\right). \quad (2)$$

Governing Equations

Generally, the main governing equations of Flow-3D software are continuity and momentum equations in 3 dimensions of (x, y, z). The continuity equation show as below [19]:

$$V_F \frac{\partial \rho}{\partial t} + \frac{\partial}{\partial x}(\rho u A_x) + R \frac{\partial}{\partial y}(\rho v A_y) + \frac{\partial}{\partial z}(\rho w A_z) + \xi \frac{\rho u A_x}{x} = R_{DIF} + R_{SOR}, \quad (3)$$

where V_F is the fractional volume open to flow, ρ is the density of fluid, RDIF is a turbulent diffusion term, and RSOR is a mass source. The velocity components (u, v, w) are in the coordinate directions (x, y, z) or (r, θ , z). A_x, A_y and A_z are the fractional area open to flow in the x, y and z-direction, respectively. The coefficient R depends on the choice of coordinate system in the following way. Other information is related to this equation can be find somewhere else [19].

General momentum equations which are used in the Flow-3D software are show as below in the three dimensions (Eqs. (4)–(6)). In Eqs. (4)–(6), (G_x, G_y, G_z) are body accelerations, (f_x, f_y, f_z) are viscous accelerations, (b_x, b_y, b_z) are flow losses in porous media or across porous baffle plates, and the final terms account for the injection of mass at a source represented by a geometry component [19]. The term $U_w = (u_w, v_w, w_w)$ is the velocity of the source component, which will generally be non-zero for a mass source. The term $U_s = (u_s, v_s, w_s)$ is the velocity of the fluid at the surface of the source relative to the source itself. More information is related to this equation can be find somewhere else [19].

$$\frac{\partial u}{\partial t} + \frac{1}{V_F} \left\{ u A_x \frac{\partial u}{\partial x} + v A_y R \frac{\partial u}{\partial y} + w A_z \frac{\partial u}{\partial z} \right\} - \xi \frac{A_y V^2}{x V_F} = -\frac{1}{\rho} \frac{\partial p}{\partial x} + G_x + f_x - b_x - \frac{R_{SOR}}{\rho V_F} (u - u_w - \delta u_s), \quad (4)$$

$$\frac{\partial v}{\partial t} + \frac{1}{V_F} \left\{ u A_x \frac{\partial v}{\partial x} + v A_y R \frac{\partial v}{\partial y} + w A_z \frac{\partial v}{\partial z} \right\} + \xi \frac{A_y u v}{x V_F} = -\frac{1}{\rho} \left[R \frac{\partial p}{\partial y} \right] + G_y + f_y - b_y - \frac{R_{SOR}}{\rho V_F} (v - v_w - \delta v_s), \quad (5)$$

$$\frac{\partial w}{\partial t} + \frac{1}{V_F} \left\{ u A_x \frac{\partial w}{\partial x} + v A_y R \frac{\partial w}{\partial y} + w A_z \frac{\partial w}{\partial z} \right\} = -\frac{1}{\rho} \frac{\partial p}{\partial z} + G_z + f_z - b_z - \frac{R_{SOR}}{\rho V_F} (w - w_w - \delta w_s). \quad (6)$$

Intelligent Systems
MLP Model

MLP is the most famous model of artificial neural networks (ANN). Figure 2 shows a simple configuration of a feed forward three layer MLP model used in this study. Feed forward means that all the neurons are received inputs from the left hand side. Inputs of model are introduced in the first layer. It should be noted that the main process is not in the first layer, and the main process of model start by the weights and information which are exist in the joints and neurons of hidden layer. Then the hidden layer, generate outputs in the last or third layer by the transformation of inputs with an appropriate nonlinear transfer function [21].

In order to find the appropriate weights that mentioned above, the model should have a training stage. Training stage includes a learning process during which input and known output data are provided to the model and the values of the weights are adjusted to optimize the accuracy of the model output [8]. The ANN model training process was continued until the goodness of fit (e.g., the sum of squared errors)

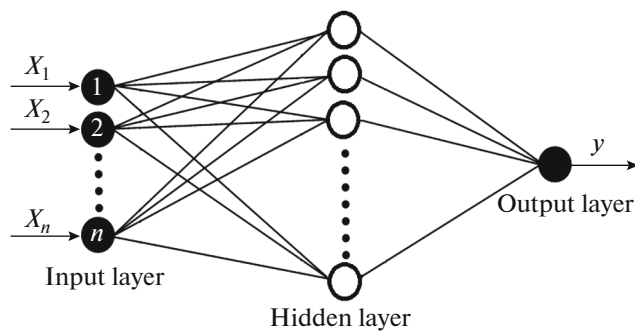


Fig. 2. Simple configuration of a feed forward three layer MLP model.

dropped below a pre-determined value or until the number of training epochs exceeded a specific value [1]. After successful training, the model was tested with a validation data set and the accuracy of the model's output was evaluated by comparing the model output with observed values.

RBF Model

This kind of artificial neural network consider a radial range around the data which each input data located in this radial range, the input data involved in the model process. Radial basis function (RBF) model always has three layers in its configuration. These three layers are named as input, hidden and output layer. It should be noted that the number of neurons in the hidden layer was set to the number of observation data inputs, and a Gaussian function was used as the transfer function for this layer [11]. Training stage of the RBF models are: (i) determining the basis functions of the hidden layer and (ii) determining the weights of the connections or joints to the output layer. More explanations and details of RBF models and their applications can be found elsewhere [13, 23].

GRNN Model

Generalized Regression Neural Networks (GRNN) is a kind of feed forward ANN which introduced by Specht [32] for the first time. GRNN is the back propagation probabilistic neural network which is used to estimate the continuous variables. Generally, GRNN has four layers named input, pattern, summation and output layer. The first layer is fully connected to the second, pattern layer, where each unit represents a training pattern and its output is a measure of the distance of the input from the stored patterns [14]. Each pattern layer unit is connected to the two neurons in the summation layer: S -summation neuron and D -summation neuron. This model does not need the repetitious training process and worked based on the non-linear regression theory [22].

M5P Model

Quinlan [30] is the pioneer researcher to introduce the M5P models based on the tree division method. This model is used to relate the dependent with independent variables. Besides, M5P model is used for both quantitative and qualitative data, in contrast with decision tree model which used just for qualitative data [30, 31]. M5P model is similar to the Piece-wise linear functions which is a combination of linear regression and tree regression that has a numerous application in various fields of study. Regression model present a regression equation for space of total data, while the tree regression model divide data set to some subsets which named leaves. Then, introduce a numerical label to each leaf. Replacing the linear regression equation by this label to predict continues variables is the task that M5P is done. Structure of decision tree is like a tree that consist of root, branches, nodes and leaves which are drawn from up to down. In other words, root is the first node which is located at the top, and a chain of nodes and branches links to reach the leaves. Branches consist of a numerical range which start from parent nodes and end to the child node. In the M5P model, there are two branch crotches from each parent node.

Developing of decision tree is started with dividing the data to some branches and crotches. This division is done by maximizing the reduction in standard deviation of data in child node. While the reduction in standard deviation of data in child node is not possible, the parent node is not divided and no leaf is developed in the last node. The reduction in standard deviation of child node (SDR) is calculated from the below equation [29]:

$$SDR = sd(T) - \sum \frac{|T_i|}{|T|} sd(T_i), \quad (7)$$

where T is the input data to the parent node, T_i is the subset of input data to the parent node and sd is the standard deviation.

RESULTS AND DISCUSSION

According to the importance of combined weir-gate structure which explained in the Introduction, this section start with simulating the flow over the combined triangular weir-rectangular gate structure and then follow by evaluating the effect of dimensionless parameters on the discharge coefficient. Then, four intelligent systems models (MLP, RBF, GRNN and M5P) prepared to estimate the discharge coefficient. The results of these models evaluate and compare with each other by doing comprehensive accuracy analyses.

Physical Model versus Numerical Model

In this study, by considering the RNG model and discharge as a boundary condition; four combined weir-gate structure simulated with different geometry. These four different weir-gate structures named as model 1 to 4, and the details of them are as below:

Model 1: with gate width of 0.05 m, gate height of 0.0125 m and y of 0.27 m.

Model 2: with gate width of 0.05 m, gate height of 0.025 m and y of 0.26 m.

Model 3: with gate width of 0.05 m, gate height of 0.0375 m and y of 0.24 m.

Model 4: with gate width of 0.05 m, gate height of 0.05 m and y of 0.23 m.

Figure 3 shows a 3D view of a sample weir-gate simulation. In the simulator like to the laboratory, at the starting time the water comes into the flume till reach the final elevation at the upstream of structure and the model and flow were stable and steady. It should be noted that the results of this study are in steady flow. Differences between steady and unsteady flow were discussed in the literature [6, 7].

Figures 4a–4d show a comparison of water head (h) of numerical model versus physical model for model 1 to 4, respectively. The points in these figures are represents for various discharges. According to these figures, the R^2 are 0.996, 0.989, 0.987 and 0.986, respectively for model 1 to 4. These values of correlation coefficient show that the accuracy of results for all models are good and the numerical model works very well in simulation the water head over the combined structure. Therefore, it can be concluded that the Flow-3D is applicable in simulation of flow over the triangular weir-rectangular gate, in this study.

Figures 5a–5d show the variation of numerical discharge coefficient with discharge for model 1 to 4, respectively. It is obvious in this figure that in all models, the discharge coefficient decreases as discharge increase. Moreover, the range of discharge coefficient is (0.31–0.78), (0.28–0.9), (0.32–0.56) and (0.35–0.86) for model 1 to 4, respectively. Hence, the range of discharge coefficient of combined triangular weir-rectangular gate of this study is between (0.3–0.9), respectively.

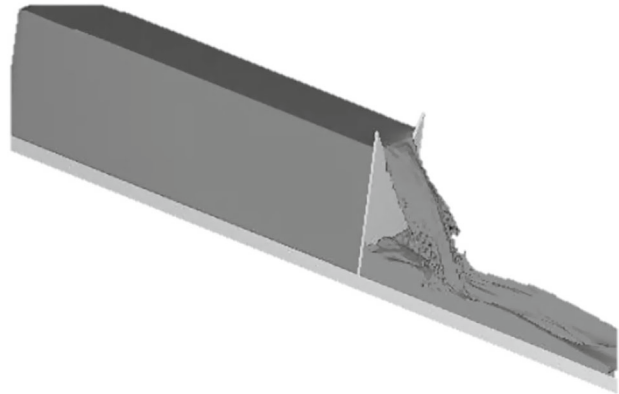


Fig. 3. 3D view of a sample weir-gate simulation.

Table 1 shows the results of goodness of fit (RMSE, MAE and MARE) for discharge coefficient (C_d) and water head (h) of model 1 to 4 and all models data. One can observe in the Table 1 that the values of RMSE, MAE and MARE for model 1 to 4 and all models are good for both discharge coefficient and water head. In more details, the RMSE, MAE and MARE of all models are 0.0673, 0.221 and 0.295 for discharge coefficient and 0.0041, 0.061 and 0.184 for water head, respectively; which show a high accuracy in estimation of discharge coefficient, water head and applicability of Flow-3D software.

Effect of Non-Dimensional Parameters on C_d

Based on the dimensional analyses which explained before, the discharge coefficient of present study is related to three non-dimensional parameters of h/b , h/d and h/y . In this section, try to evaluate the effect of these non-dimensional parameters on discharge coefficient by using the numerical data. Figure 6 shows the variation of numerical discharge coefficient with h/b , h/d and h/y for model 2. One can observe from Fig. 7 that by increasing the dimensionless parameters (h/b , h/d and h/y), the discharge coefficient decreases. In other words, there is inverse relation between the C_d and the effective non-dimensional parameters in this study.

Table 1. Results of goodness of fit for discharge coefficient and water head of model 1 to 4 and all models data

Parameter	Goodness of fit	Model 1	Model 2	Model 3	Model 4	All models
Discharge coefficient (C_d)	RMSE	0.0674	0.0675	0.0363	0.09	0.0673
	MAE	0.225	0.223	0.168	0.261	0.221
	MARE	0.311	0.29	0.256	0.321	0.295
Water head (h)	RMSE	0.0036	0.0042	0.0037	0.0049	0.0041
	MAE	0.058	0.061	0.057	0.065	0.061
	MARE	0.193	0.185	0.158	0.195	0.184

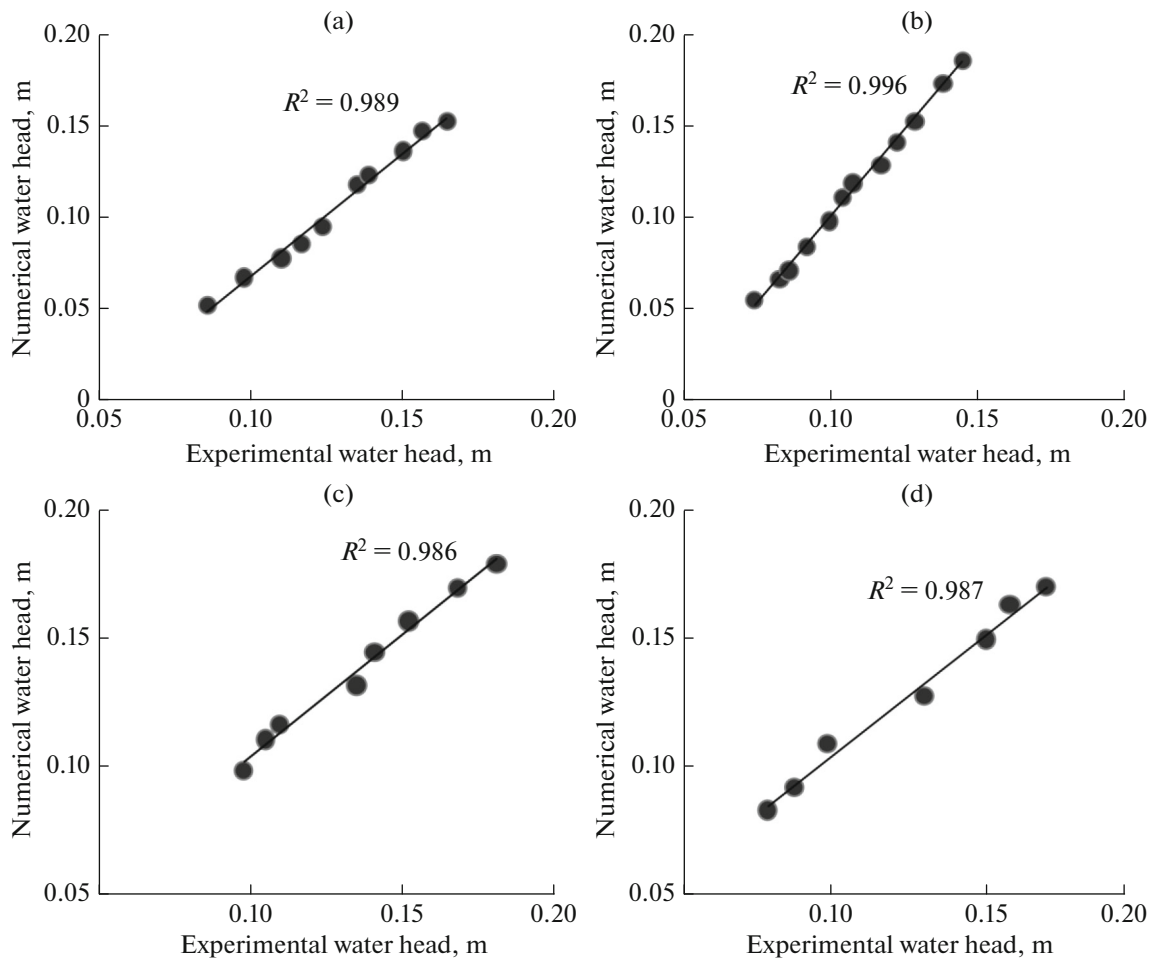


Fig. 4. Comparison of water head (h) of numerical versus physical model for model 1 to 4 (a–d).

Intelligent Systems

Based on the objectives of this study and the high efficiency of intelligent systems in estimation of hydraulic parameters, four intelligent system models (MLP, RBF, GRNN and MSP) prepared to estimate discharge coefficient of combined triangular weir-rectangular gate. It should be noted that the input parameters to the models are h/b , h/d and h/y ; and the output is the discharge coefficient (Cd). Moreover, the procedure of runs of each model is using the train data set for training the model and then using the validation data set to validate and test the results. Hence, 70% of data used as a train stage and the rest 30% of total data used as a validation stage. In the following, the results of these models were evaluated and compared with each other to find the superior model in this study.

MLP Model

Brief explanations about the MLP exist in the Materials and Methods section. In this study, after so many trial and errors a MLP model with three layer

and 11 neurons in the hidden layer were choose. Figure 7 shows the predicted discharge coefficient versus the observed one for MLP model. It is obvious from this figure that the results are very good and MLP model can predict Cd with high accuracy ($R^2 = 0.958$).

RBF Model

Brief explanations about the Radial Basis Function (RBF) exist in the Materials and Methods section. In this study, after so many trial and errors a RBF model with radial of 8 and 9 neurons were choose. Figure 8 compared the predicted discharge coefficient with the observed one for RBF model. One can see from this figure that the results are very good and RBF model can predict Cd well ($R^2 = 0.85$). However, the correlation coefficient of MLP model is better than RBF.

GRNN Model

Brief explanations about the Generalized Regression Neural Networks (GRNN) exist in the Materials

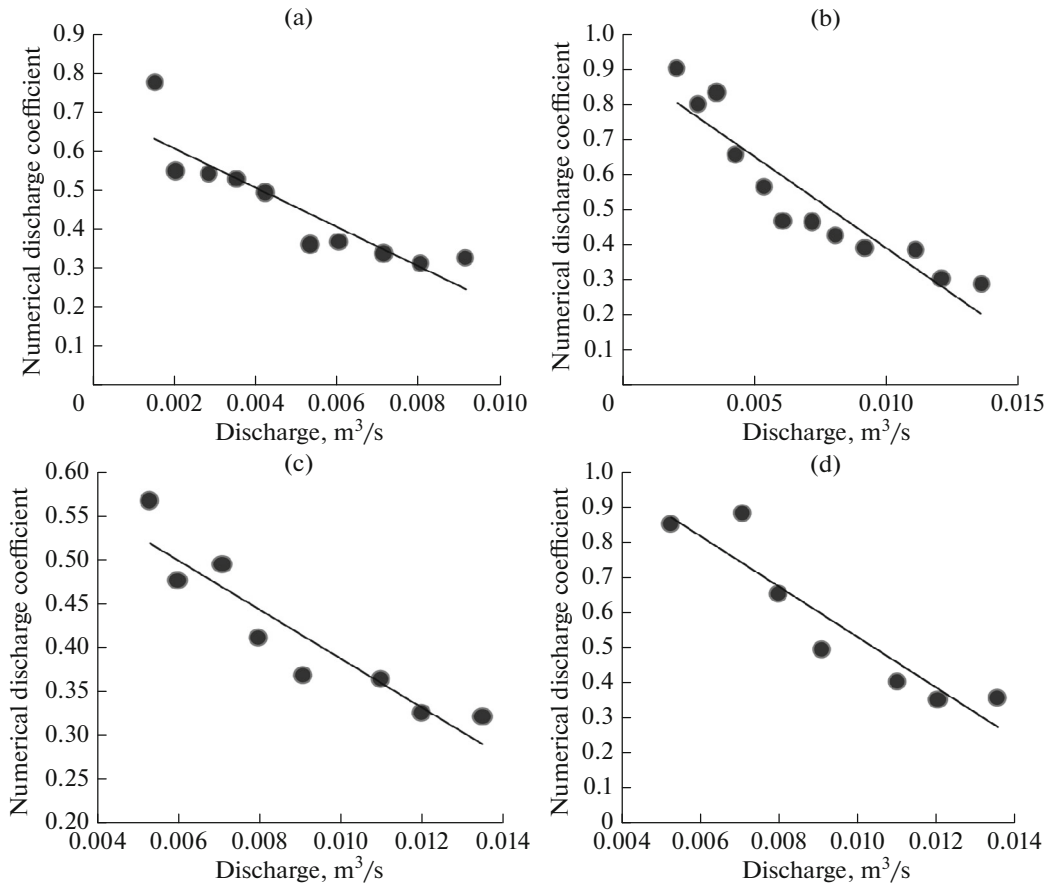


Fig. 5. Variation of numerical discharge coefficient with discharge for model 1 to 4 (a–d).

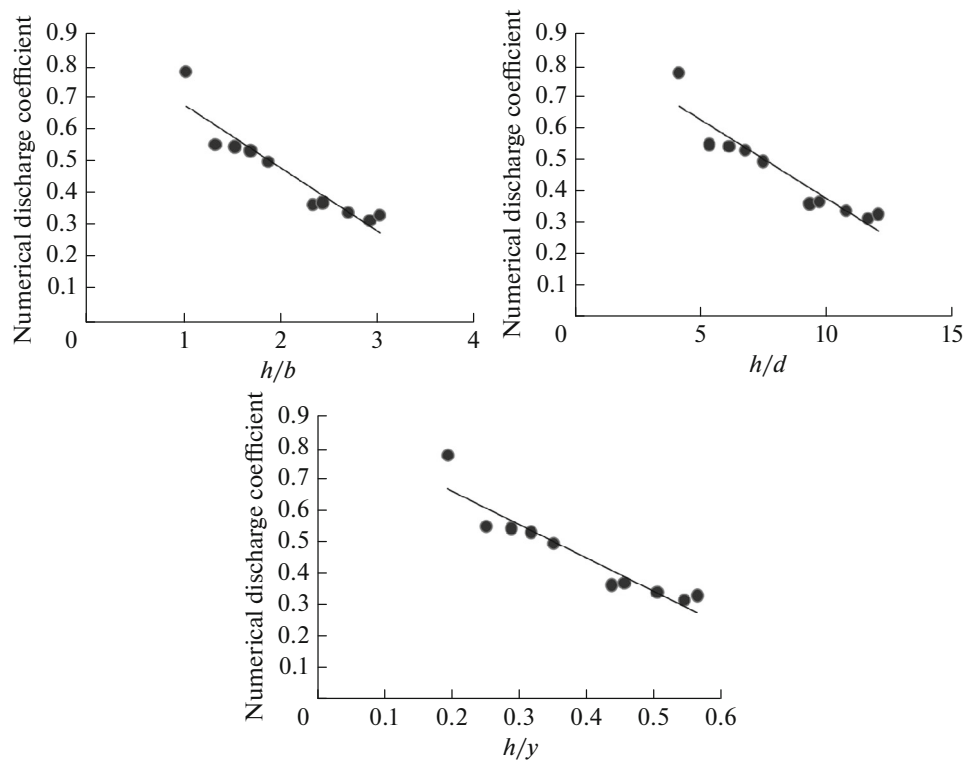


Fig. 6. Variation of numerical discharge coefficient with h/b , h/d and h/y for model 2.

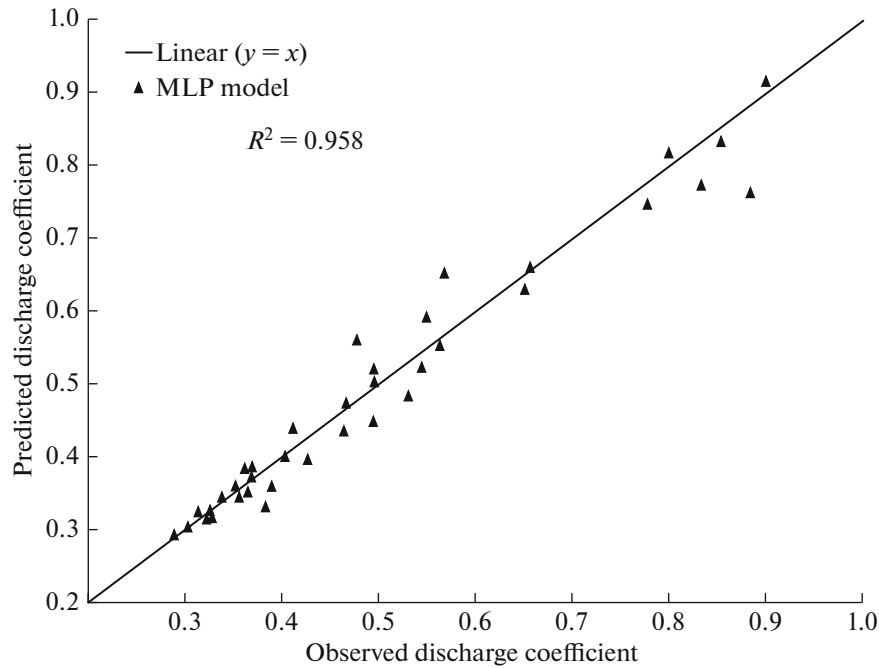


Fig. 7. Predicted versus the observed discharge coefficient for MLP model.

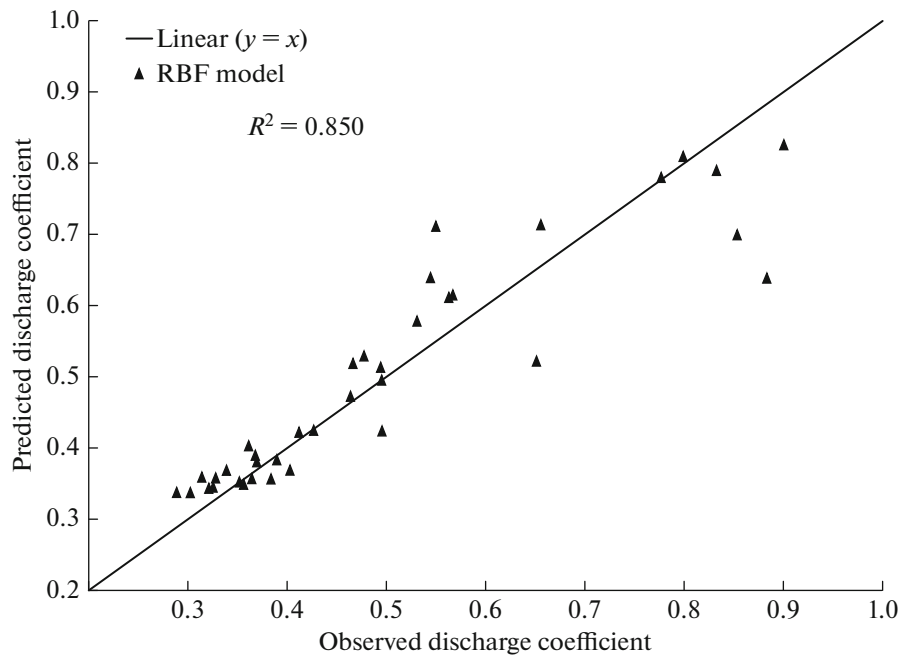


Fig. 8. Predicted versus the observed discharge coefficient for RBF model.

and Methods section. Figure 9 shows the predicted discharge coefficient versus the observed one for GRNN model. One can see from this figure that the results are good and GRNN model can predict Cd well ($R^2 = 0.837$). However, the correlation coefficient of MLP model is better than GRNN.

M5P Model

Brief explanations about the tree model (M5P) exist in the Materials and Methods section. According to the data used in this study, M5P model makes a tree with two branches. Figure 10 shows the predicted discharge coefficient versus the observed one for M5P

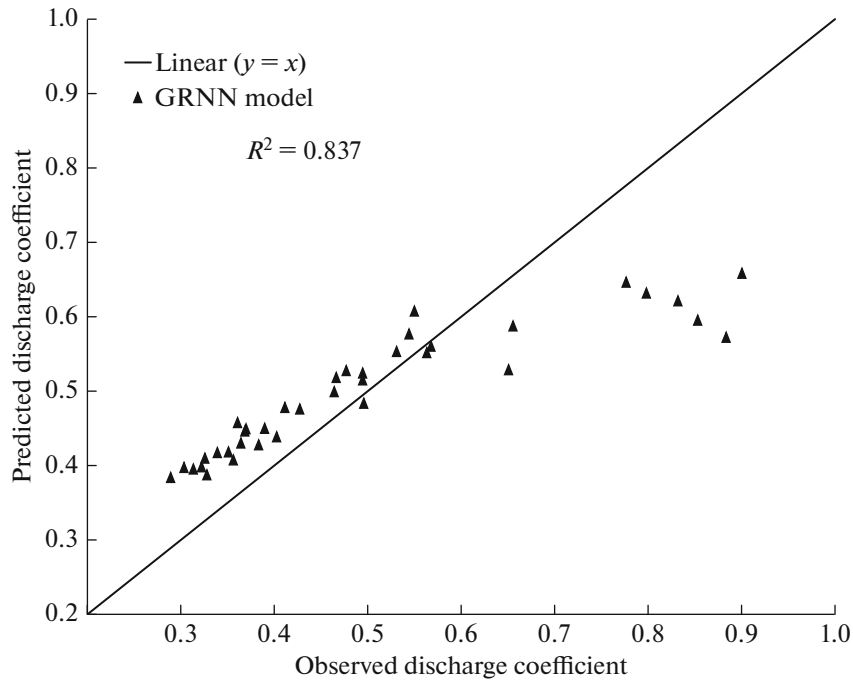


Fig. 9. Predicted versus the observed discharge coefficient for GRNN model.

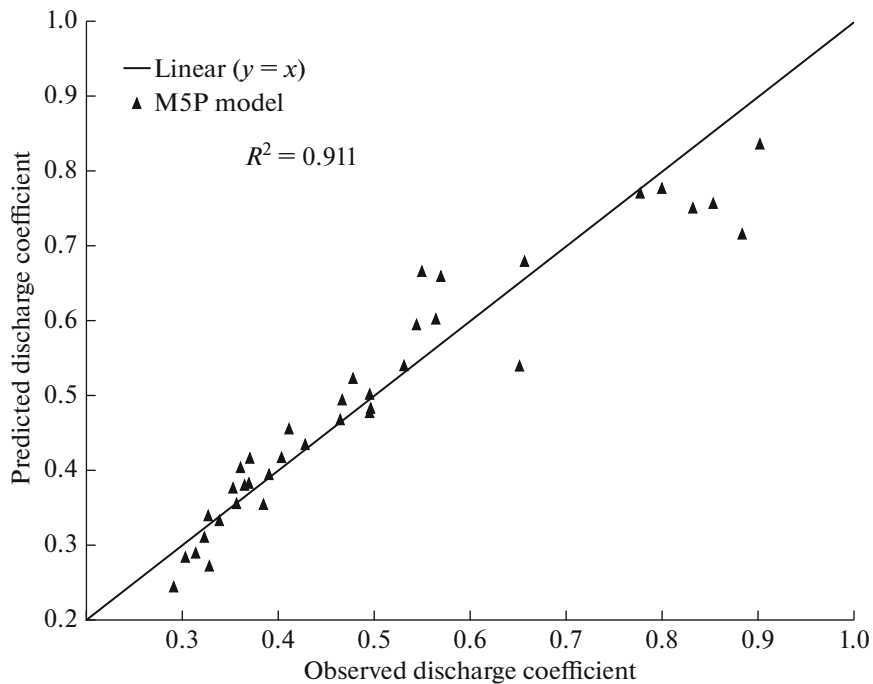


Fig. 10. Predicted versus the observed discharge coefficient for M5P model.

model. It is obvious from this figure that the results are very good and M5P model can predict Cd with high accuracy ($R^2 = 0.911$). Although the correlation coefficient of M5P better than RBF and GRNN. But, the MLP correlation coefficient is better than GRNN.

Superior Model

In order to find the superior models in this study accuracy analyses and comparison of results with each other are needed. As mentioned before, all models used in this study (MLP, RBF, GRNN and M5P) has

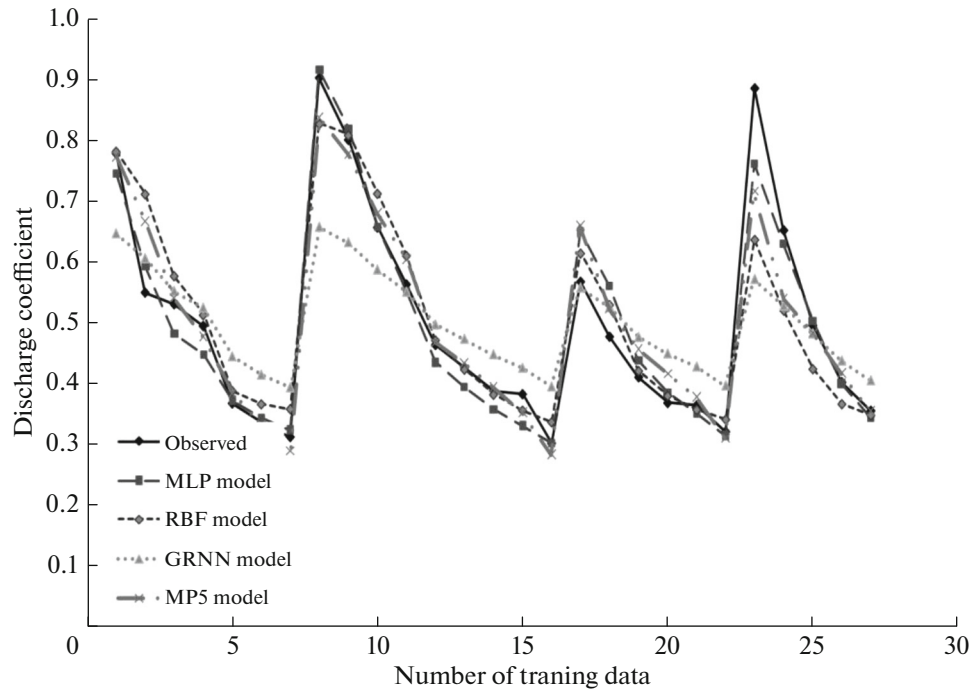


Fig. 11. Comparison between the observed Cd with the results of MLP, RBF, GRNN and M5P models in training stage.

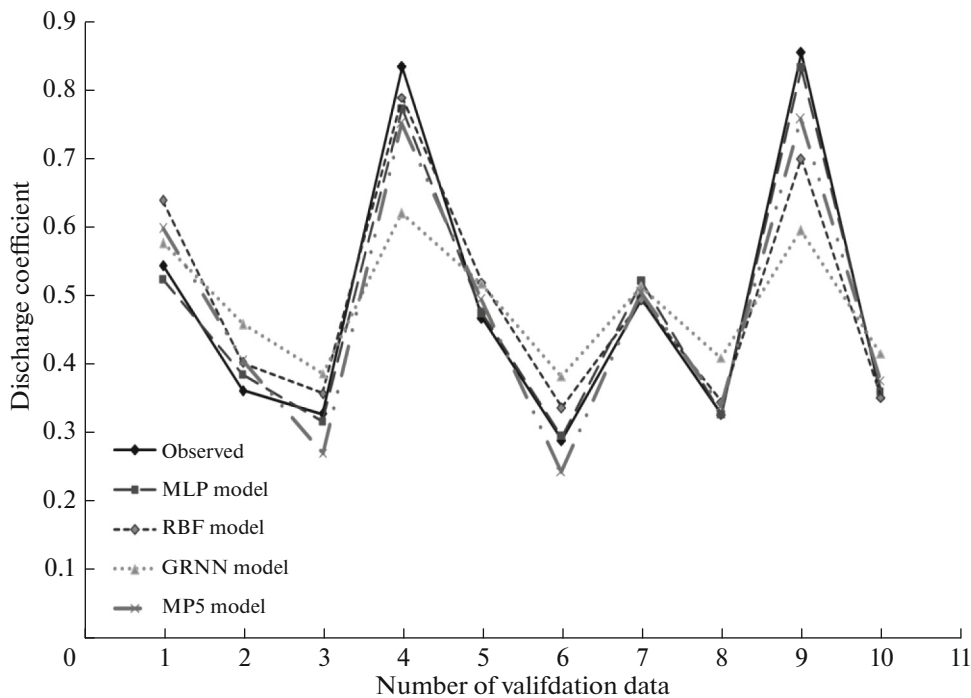


Fig. 12. Comparison between the observed Cd with the results of MLP, RBF, GRNN and M5P models in validation stage.

both training and validation stage. Therefore, evaluating the accuracy analyses in training, validation and total data set for all models are important. Figure 11 compared the observed discharge coefficients of triangular weir-rectangular gate with the results of MLP, RBF, GRNN and M5P models in training stage. One

can see from this figure that the MLP model matched better than others with observed data and GRNN is not impressive in compare with other models.

As the validation stage is more important than training stage for testing the applicability of models; Fig. 12 drawn for comparing the observed discharge

Table 2. Accuracy analyses for training, validation and total data sets for all models

Model	Data set	Statistical index					Total ranking
		R^2 , %	MAE	MARE, %	RMSE	NSE	
MLP	Training	95.5	0.029	5.62	0.04	0.944	5
	Ranking	1	1	1	1	1	
	Validation	99.1	0.019	3.5	0.025	0.997	
	Ranking	1	1	1	1	1	
	Total	95.8	0.026	5.04	0.037	0.984	
	Ranking	1	1	1	1	1	
RBF	Training	82.9	0.045	8.56	0.071	0.829	16
	Ranking	4	3	3	3	3	
	Validation	91.4	0.048	9.07	0.065	0.982	
	Ranking	3	3	2	3	3	
	Total	85	0.046	8.7	0.069	0.943	
	Ranking	3	3	3	3	3	
GRNN	Training	83.4	0.078	15.3	0.103	0.733	19
	Ranking	3	4	4	4	4	
	Validation	84.9	0.097	19.3	0.122	0.936	
	Ranking	4	4	4	4	4	
	Total	83.7	0.083	16.38	0.109	0.86	
	Ranking	4	4	4	4	4	
M5P	Training	90	0.036	6.61	0.054	0.9	10
	Ranking	2	2	2	2	2	
	Validation	93.8	0.045	10.03	0.053	0.988	
	Ranking	2	2	3	2	2	
	Total	91.1	0.038	7.53	0.054	0.966	
	Ranking	2	2	2	2	2	

coefficient with MLP, RBF, GRNN and M5P results in validation stage. Similar to the training stage, it can be concluded from this figure that the MLP model matched better than others with observed data and the GRNN results is not impressive in compare with other models.

Figures 11 and 12 show the visual comparison of training and validation data sets of models. In order to evaluate and compare the models in more details, the accuracy analyses by using various statistical indices were done and represent in Table 2. These statistical indices are R^2 , Mean Absolute Error (MAE), Mean Absolute Relative Error (MARE), Root Mean Square Error (RMSE) and Nash–Sutcliffe Efficiency (NSE). It should be noted that if the values of MAE, MARE and RMSE are near to zero, and if the values of NSE and R^2 are near to one (or 100 if representing as percentage); it means the result are more accurate. Besides, in order to evaluate the results in a better way, the ranking scheme is choose. The best results in the

ranking scheme received a first ranking number (i.e. 1) and the worst one is the last ranking number (i.e. 4 in this study); and other results sorted between 1 and 4 based on their accuracy.

One can be seen in Table 2 that the MLP model has the best results in training, validation and total data sets by ranking number of 5 for all of them. After that, M5P show the best result with ranking number of 10, 11 and 10 for training, validation and total data sets, respectively. Then, the third place belongs to the RBF model by having the ranking number of 16, 14 and 15 for training, validation and total data sets, respectively. And in the last place, GRNN exist with the ranking number of 19, 20 and 20 for training, validation and total data sets, respectively. Therefore, based on the comprehensive accuracy analyses, one can suggest the MLP model as the superior intelligent system model and GRNN as the poorest one among other models to predict discharge coefficient of triangular weir-rectangular gate in this study.

CONCLUSIONS

In this study, based on the importance of combined weir-gate structure, flow over four combined triangular weir-rectangular gate simulated with different geometry via Flow-3D software. Then, dimensional analyses were done and three effective non-dimensional parameters of h/b , h/d and h/y were introduced to the four intelligent system models (MLP, RBF, GRNN and M5P) as input to predict C_d as output. The total data set divided into two parts as 70% for training stage and 30% for validation stage. Then, by doing a comprehensive accuracy analyses with computing the statistical indices (R^2 , MAE, MARE, RMSE and NSE), results were evaluated and compared with each other. Hence, the following bullets can represent as conclusion of results:

By comparing the results of water head and discharge coefficient of experimental data with numerical model, one can be concluded that the Flow-3D is applicable in simulation of flow over the triangular weir-rectangular gate, in this study.

It is obvious in this figure that in all models the discharge coefficient decreases as discharge increase. Moreover, the range of discharge coefficient is (0.3–0.9) in this study.

Increasing the effective dimensionless parameters (h/b , h/d and h/y), decreased the discharge coefficient. In other words, there is inverse relation between the C_d and the effective non-dimensional parameters in this study.

Results of evaluating the intelligent systems by accuracy analyses show that models used in this study can be sort due to the accuracy in estimating discharge coefficient as MLP, M5P, RBF and GRNN, respectively (by ranking number of 5, 10, 16 and 19, respectively).

The superior model in this study is MLP for estimating discharge coefficient of triangular weir-rectangular gate.

REFERENCES

1. Abidin, K., Artificial neural network study of observed pattern of scour depth around bridge piers, *Comput. Geotech.*, 2010, vol. 37, no. 3, pp. 413–418. <https://doi.org/10.1016/j.compgeo.2009.10.003>
2. Ahmed, F.H., Characteristics of discharge of the combined flow through sluice gates and over weirs, *J. Eng. Techn.*, Iraq, 1985, vol. 3, no. 2, pp. 49–63. (in Arabic)
3. Alhamid, A.A., Husain, D., and Negm, A.M., Discharge equation for combined flow over rectangular weirs and below inverted triangular weirs, *Arab Gulf J. Sci. Res.*, 1996, vol. 14, no. 3, pp. 595–607.
4. Alhamid, A.A., Negm, A.M., and Al-Brahim, A.M., Discharge equation for proposed self-cleaning device, *J. King Saud Univ.*, 1997, vol. 91, pp. 13–24.
5. Amini, N., Balouchi, B., and Shafai Bejestan, M., Reduction of local scour at river confluences using collar, *J. Sediment. Res.*, 2017, vol. 32, no. 3, pp. 364–372.
6. Balouchi, B., Abedini, M.J., and Manhart, M., A simulation-optimization technique to estimate discharge in open channels based on water level data alone—Gradually Varied Flow condition, *IJSTC Journal*, Springer, 2018, vol. 43, no. 8, pp. 1–15. <https://doi.org/10.1007/s40996-018-0149-5>
7. Balouchi, B. and Abedini, M.J., System identification and subsequent discharge hydrograph estimation in waterway corridors based on water level data alone—Unsteady flow condition, *J. Hydrol. Engin.*, ASCE, 2019, vol. 24, no. 10. [https://doi.org/10.1061/\(ASCE\)HE.1943-5584.0001848](https://doi.org/10.1061/(ASCE)HE.1943-5584.0001848)
8. Balouchi, B., Nikoo, M.R., and Adamowski, J., Development of expert systems for the prediction of scour depth under live-bed conditions at river confluences: Application of different types of ANNs and the M5P model tree, *Appl. Soft Comp. J.*, 2015, vol. 34, pp. 51–59.
9. Balouchi, B. and Rakhshanderoo, G.R., Using physical and soft computing models to evaluate discharge coefficient for combined weir gate structures under free flow condition, *IJST Journal*, 2018, vol. 42, no. 1. <https://doi.org/10.1007/s40996-018-0117-0>
10. Balouchi, B. and Shafai Bajestan, M., The effect of bed load on maximum scour depth at river confluence, *Ecol., Environ. Conserv.*, 2011, vol. 18, no. 1, pp. 157–164.
11. Bateni, S.M., Borghei, S.M., and Jeng, D.S., Neural network and neuro-fuzzy assessments for scour depth around bridge piers, *J. Eng. Appl. Artif. Intel.*, 2007, vol. 20, no. 3, pp. 401–414. <https://doi.org/10.1016/j.engappai.2006.06.012>
12. Bilhan, O., Emiroglu, M.E., and Kisi, O., Use of artificial neural networks for prediction of discharge coefficient of triangular labyrinth side weir in curved channels, *Adv. Engin. Soft.*, 2011, vol. 42, pp. 208–214.
13. Cheng, M.Y., Cao, M.T., and Wu, Y.W., Predicting equilibrium scour depth at bridge piers using evolutionary radial basis function neural network, *J. Comput. Civil Eng.*, 2014, vol. 29, no. 5, 04014070. [https://doi.org/10.1061/\(ASCE\)CP.1943-5487.0000380](https://doi.org/10.1061/(ASCE)CP.1943-5487.0000380)
14. Cigizoglu, H.K., Artificial neural networks in water resources, *Integr. Inf. Environ. Security*, 2008, pp. 115–148. https://doi.org/10.1007/978-1-4020-6575-0_8
15. Dehghani, A.A., Bashiri, H., Meshkati, E., Ahadpoor, A., Experimental investigation of scouring in downstream of combined flow over weirs and below gates, *33rd IAHR Conf.*, Canada, 2009, pp. 3604–3609.
16. El-Saiad, A.A., Negm, A.M., and Waheed El-Din, U., Simultaneous flow over weirs and below gates, *Civil Eng. Res. Mag.*, 1995, vol. 17, no. 7, pp. 62–71.
17. Emiroghlu, M.E., Bilhan, O., and Kisi, O., Neural networks for estimation of discharge capacity of triangular

- labyrinth side-weir located on a straight channel, *Expert Syst. Applic.*, 2011, vol. 38, pp. 867–874.
18. Ferro, V., Simultaneous flow over and under gate, *J. Irrig. Drain. Eng.*, 2000, vol. 126, no. 3, pp. 190–193.
 19. Flow-3D, *User manual*, Flow Science Inc., 2008.
 20. Juma, I.A., Hussein, H.H., and Al-Sarraj, M.F., Analysis of hydraulic characteristics for hollow semi-circular weirs using artificial neural networks, *Flow Meas. Instrum.*, 2014, vol. 38, pp. 49–53.
 21. Lee, T.L., Jeng, D.S., Zhang, G.H., and Hong, J.H., Neural network modeling for estimation of scour depth around bridge piers, *J. Hydro Dyn.*, 2007, vol. B19, no. 3, pp. 378–386.
[https://doi.org/10.1016/S1001-6058\(07\)60073-0](https://doi.org/10.1016/S1001-6058(07)60073-0)
 22. Li, C.F., Zhang, J.B., and Wang, S.T., Comparative study on input-expansion-based improved general regression neural network and Levenberg-Marquardt BP network, *Lecture Notes in Computer Sci.*, 2006, vol. 4113, pp. 83–93.
 23. López-Martín, C., Predictive accuracy comparison between neural networks and statistical regression for development effort of software projects, *Appl. Soft Comput.*, 2015, vol. 27, pp. 434–449.
<https://doi.org/10.1016/j.asoc.2014.10.033>
 24. Mohamed, H.I., Abozeid, G., and Shehata, S.M., Hydraulics of clear and submerged overfall weirs with bottom circular openings, *Ain Shams Eng. J.*, 2011, vol. 1, no. 2, pp. 115–119.
<https://doi.org/10.1016/j.asej.2011.03.004>
 25. Negm, A.M., Characteristics of combined flow over weirs and under gate with unequal contractions, *Proc. 2nd Int. Conf. on Hydro-Sci. Engineering*, Beijing, China, 1995, vol. 2, no. A, pp. 285–292.
 26. Negm, A.M., Al-barahim, A.M., and Al-hamid, A.A., Combined free flow over weirs and gate, *J. Hydraulic Res.*, 2002, vol. 40, no. 3, pp. 359–365.
 27. Negm, A.M., El-Saiad, A.A., Alhamid, A.A., and Husain, D., Characteristics of simultaneous flow over weir and below inverted V-Notches, *Civil Engin. Res. Magazine (CERM)*, 1994, vol. 16, no. 9, pp. 786–799.
 28. Negm, A.M., El-Saiad, A.A., and Saleh, O.K., Characteristics of combined flow over weirs and below submerged gates, *Proc. of Al-Mansoura engineering 2nd Int. Conf. MEIC'97*, 1–3 April, Faculty of Engineering, Al-Mansoura Univ., Al-Mansoura, Egypt, 1997, vol. III, no. B, pp. 259–272.
 29. Pal, M. and Deswal, S., M5 model tree based modeling of reference evapotranspiration, *Hydrol. Processes*, 2009, vol. 23, pp. 1437–1443.
 30. Quinlan, J.R., Introduction of decision trees, *Machine learning*, 1986, vol. 1, pp. 81–106.
 31. Quinlan, J.R., Learning with continuous classes, *Proceedings of the Fifth Australian Joint Conf. Artificial Intelligence*, Hobart, Australia, World Scientific, Singapore, 1992, pp. 343–348.
 32. Specht, D.F., A General Regression Neural Network, *IEEE Trans. Neural Netw.*, 1991, vol. 2, no. 6, pp. 568–576.